2-10-2022

Second Heart Field–Derived Cells Contribute to Angiotensin II–Mediated Ascending Aortopathies

Hisashi Sawada
University of Kentucky

Yuriko Katsumata
University of Kentucky

Hideyuki Higashi

Chen Zhang
Baylor College of Medicine

Yanming Li
Baylor College of Medicine

See next page for additional authors

Second Heart Field–Derived Cells Contribute to Angiotensin II–Mediated Ascending Aortopathies

Digital Object Identifier (DOI)
https://doi.org/10.1161/CIRCULATIONAHA.121.058173

Authors
Hisashi Sawada, Yuriko Katsumata, Hideyuki Higashi, Chen Zhang, Yanming Li, Stephanie Morgan, Lang H. Lee, Sasha A. Singh, Jeff Z. Chen, Michael K. Franklin, Jessica J. Moorleghen, Deborah A. Howatt, Debra L. Rateri, Ying H. Shen, Scott A. LeMaire, Masanori Aikawa, Mark W. Majesky, Hong S. Lu, and Alan Daugherty

Circulation

ORIGINAL RESEARCH ARTICLE

Second Heart Field–Derived Cells Contribute to Angiotensin II–Mediated Ascending Aortopathies

Hisashi Sawada, MD, PhD; Yuriko Katsumata, PhD; Hideyuki Higashi, MS; Chen Zhang, MD; Yanming Li, PhD; Stephanie Morgan, PhD; Lang H. Lee, PhD; Sasha A. Singh, PhD; Jeff Z. Chen, PhD; Michael K. Franklin, MS; Jessica J. Moorleghen, BS; Deborah A. Howatt, BS; Debra L. Rateri, BS; Ying H. Shen, MD, PhD; Scott A. LeMaire, MD; Masanori Aikawa, MD, PhD; Mark W. Majesky, PhD; Hong S. Lu, MD, PhD; Alan Daugherty, PhD, DSc

BACKGROUND: The ascending aorta is a common location for aneurysm and dissection. This aortic region is populated by a mosaic of medial and adventitial cells that are embryonically derived from either the second heart field (SHF) or the cardiac neural crest. SHF-derived cells populate areas that coincide with the spatial specificity of thoracic aortopathies. The purpose of this study was to determine whether and how SHF-derived cells contribute to ascending aortopathies.

METHODS: Ascending aortic pathologies were examined in patients with sporadic thoracic aortopathies and angiotensin II (AngII)–infused mice. Ascending aortas without overt pathology from AngII-infused mice were subjected to mass spectrometry–assisted proteomics and molecular features of SHF-derived cells were determined by single-cell transcriptomic analyses. Genetic deletion of either *Lrp1* (low-density lipoprotein receptor–related protein 1) or *Tgfbr2* (transforming growth factor–β receptor type 2) in SHF-derived cells was conducted to examine the effect of SHF-derived cells on vascular integrity.

RESULTS: Pathologies in human ascending aortic aneurysmal tissues were predominant in outer medial layers and adventitia. This gradient was mimicked in mouse aortas after AngII infusion that was coincident with the distribution of SHF-derived cells. Proteomics indicated that brief AngII infusion before overt pathology occurred evoked downregulation of smooth muscle cell proteins and differential expression of extracellular matrix proteins, including several LRP1 ligands. LRP1 deletion in SHF-derived cells augmented AngII-induced ascending aortic aneurysm and rupture. Single-cell transcriptomic analysis revealed that brief AngII infusion decreased *Lrp1* and *Tgfbr2* mRNA abundance in SHF-derived cells and induced a unique fibroblast population with low abundance of *Tgfbr2* mRNA. SHF-specific *Tgfbr2* deletion led to embryonic lethality at E12.5 with dilatation of the outflow tract and retroperitoneal hemorrhage. Integration of proteomic and single-cell transcriptomics results identified PAI1 (plasminogen activator inhibitor 1) as the most increased protein in SHF-derived smooth muscle cells and fibroblasts during AngII infusion. Immunostaining revealed a transmural gradient of PAI1 in both ascending aortas of AngII-infused mice and human ascending aneurysmal aortas that mimicked the gradient of medial and adventitial pathologies.

CONCLUSIONS: SHF-derived cells exert a critical role in maintaining vascular integrity through LRP1 and transforming growth factor–β signaling associated with increases of aortic PAI1.

Key Words: angiotensin ■ aortic aneurysm, thoracic ■ fibroblast ■ mice ■ smooth muscle

Thoracic aortopathies are a spectrum of lethal diseases associated with aneurysm, dissection, and rupture.[1,2] These diseases have devastating consequences, but medical therapy has limited efficacy. Therefore, there is an urgent need to investigate mechanisms of thoracic aortopathies to facilitate development of effective therapeutics.

Correspondence to: Hisashi Sawada, MD, PhD, Saha Cardiovascular Research Center, University of Kentucky, 741 South Limestone Street, BBSRB, B251, Lexington, KY 40536; or Alan Daugherty, PhD, DSc, Saha Cardiovascular Research Center, University of Kentucky, 741 South Limestone Street, BBSRB, B243, Lexington, KY 40536. Email hisashi.sawada@uky.edu or alan.daugherty@uky.edu

Supplemental Material is available at https://www.ahajournals.org/doi/suppl/10.1161/CIRCULATIONAHA.121.058173.

For Sources of Funding and Disclosures, see page 999.

Circulation is available at www.ahajournals.org/journal/circ

Clinical Perspective

What Is New?

- Second heart field–derived smooth muscle cells and fibroblasts associate with angiotensin II–induced aortic pathologies.
- Angiotensin II induces a distinct fibroblast subcluster that is less abundant for mRNAs related to major extracellular components and transforming growth factor–β ligands and receptors but more abundant for proliferative genes.
- TGFBR2 (transforming growth factor–βreceptor type 2) deletion in second heart field–derived cells is embryonically lethal with substantial dilatation of the outflow tract in mice.
- Second heart field–specific deletion of LRP1 (low-density lipoprotein receptor–related protein 1) leads to aortic pathologies in mice, supporting the importance of second heart field–derived cells in maintaining ascending aortic wall integrity.

What Are the Clinical Implications?

- Heterogeneity of the embryonic origins of smooth muscle cells and fibroblasts contributes to complex mechanisms of vasculopathy formation, which should be considered when investigating the pathogenesis of thoracic aortopathies.

Nonstandard Abbreviations and Acronyms

AngII	angiotensin II
CNC	cardiac neural crest
Col3a1	collagen type III alpha 1 chain
Col5a2	collagen type V α2 chain
Ctsb	cathepsin B
DEG	differentially expressed gene
ECM	extracellular matrix
Eln	elastin
Fn1	fibronectin 1
LRP1	low-density lipoprotein receptor–related protein 1
Ltbp2	latent TGF-β binding protein 2
Mmp2	matrix metalloproteinase 2
PAI1	plasminogen activator inhibitor 1
scRNAseq	single-cell RNA sequencing
SHF	second heart field
SMC	smooth muscle cell
TAA	thoracic aortic aneurysm
TGF-β	transforming growth factor–β
Tgfbr2	transforming growth factor–β receptor type 2
Thbs1	thrombospondin 1
Tnc	tenascin C

Aortopathies occur throughout the thoracic aorta, with the ascending aorta being a frequently affected region.[3,4] Aortic remodeling, including medial and adventitial thickening, is a histologic feature of thoracic aortopathies that shows a transmedial gradient toward the outer medial layers and the adjacent adventitia.[5–10] Therefore, thoracic aortopathies have regional and transmural specificities, with outer medial layers in the ascending aorta being a disease-prone location. The mechanism by which outer medial layers of the ascending aorta are prone to aortopathy remains unclear.

The major cellular components of the aortic wall are smooth muscle cells (SMCs) and fibroblasts. These 2 cell types are thought to exert a pivotal role in the pathogenesis of thoracic aortopathies.[11] SMCs in the ascending aorta are derived from 2 embryonic origins: cardiac neural crest (CNC) and second heart field (SHF).[12] Select fibroblasts are also derived from the CNC and SHF.[13] Lineage tracking studies have demonstrated that CNC- and SHF-derived SMCs occupy inner and outer medial layers of the ascending aorta, respectively.[13] The region-specific distribution of thoracic aortopathies coincides with the distribution of SMCs from the SHF origin. Therefore, we hypothesized that SHF-derived cells play an important role in ascending aortopathies. To test this hypothesis, we investigated whether SHF-derived cells colocalized with the evolution of aortic pathology produced by angiotensin II (AngII) infusion in mice and investigated the molecular basis of AngII-mediated ascending aortopathies using proteomic and single-cell transcriptomic approaches. Our findings using omics analyses were validated by 2 SHF-specific genetic deletion studies in mice.

METHODS

Additional detailed methods are presented in the Supplemental Methods. Numeric data are available in Excel Files S1–S3. All raw data and analytical methods are available from the corresponding author on appropriate request.

Human Aortic Samples

Ascending aortas were acquired from patients undergoing aortic surgery for sporadic thoracic aortic aneurysms at Baylor College of Medicine (n=10; mean age, 66±7 years; 5 male, 5 female; mean aortic diameter 5.3±0.4 cm). Aortic tissues were fixed with formalin (10% wt/vol) and incubated with ethanol (70% vol/vol), as described previously.[14] Tissues were embedded in paraffin blocks and sliced into 5-μm sections. The protocol for collecting human tissue samples was approved by the institutional review board at Baylor College of Medicine.

Mice

The following mice were purchased from The Jackson Laboratory (Table S1): ROSA26R^{LacZ} (003474), ROSA26R$^{mT/mG}$ (007676), *Lrp1* (low-density lipoprotein receptor–related

protein 1) floxed (012604), *Tgfbr2* (transforming growth factor–β receptor type 2) floxed (012603), and Wnt1-*Cre* (022501, also known as B6-Wnt1-*Cre*2). Mef2c-*Cre* mice (030262) were purchased from the Mutant Mouse Resource and Research Center. For cell tracking studies of CNC and SHF origins, either Wnt1-*Cre* or Mef2c-*Cre* male mice were bred to ROSA26R^{LacZ} female mice, respectively. For single-cell RNA sequencing (scRNAseq), Mef2c-*Cre* male mice were bred to ROSA26R$^{mT/mG}$ female mice. Mef2c-*Cre* male mice were crossbred to *Lrp1* floxed female mice to delete *Lrp1* in SHF-derived cells. Mef2c-*Cre* male mice were also used for lineage-specific deletion of *Tgfbr2* in SHF-derived cells. Because of a modest induction of AngII-induced thoracic aortic aneurysms (TAAs) in female mice, only male mice were studied.[15] All experiments were approved by the Institutional Animal Care and Use Committee at either the University of Kentucky or Baylor College of Medicine in accordance with the guidelines of the National Institutes of Health.

Subcutaneous Infusion Using an Osmotic Pump

After random assignment, saline or AngII (1000 ng/kg/min; H-1705, Bachem) was infused through a subcutaneously implanted osmotic pump (Alzet model 2001 for 3 days and model 2004 for 28 days of infusion, respectively; Durect) into male mice at 10 to 14 weeks of age.[16] Surgical staples used to close incision sites were removed 7 days after surgery. Postoperative pain was alleviated by application of topical lidocaine cream (4% wt/wt; LMX4, 0496-0882-15, Eloquest Healthcare, Inc).

Statistical Analyses

Non-omics data are presented as mean±SEM or median and 25th/75th percentiles. Normality and homogeneity of variance were assessed by Shapiro-Wilk and Brown-Forsythe tests, respectively. Because the original data of ascending aortic diameter, Western blotting for Serpine1, and collagen deposition in human TAAs did not pass Shapiro-Wilk or Brown-Forsythe tests, log transformation was applied for these data. After confirming homogeneous variances and normality, 2-group or multigroup comparisons for means were performed by 2-sided Student *t* test or 2-way analysis of variance with Holm-Sidak multiple comparison test, respectively. The log-rank test was used to compare the incidence of ascending aortic rupture between groups. Other causes of death, such as abdominal aortic rupture, were treated as censored events. $P<0.05$ was considered statistically significant. Statistical analyses were performed using SigmaPlot version 14.0 (SYSTAT Software Inc).

Statistical analyses for proteomic data were performed with R (version 4.1.0).[17] Proteins in the principal component analysis plot were clustered by k-means algorithm (k=2). Differentiated proteins, transformed by the log1p function in R, between saline and AngII were identified with a Student *t* test on the basis of the false discovery rate adjusted *P* value (Q value) with <0.05 as a threshold. Enrichment analyses for Gene Ontology (biological process) and Kyoto Encyclopedia of Genes and Genomes were performed using the clusterProfiler (4.0.2) R package.[18] Heatmaps for comparisons in the standardized protein abundance (ie, Z scores) between saline and AngII were generated for differentiated proteins related to SMC contraction, matrix metalloproteinase, transforming growth factor–β (TGF-β) signaling, and extracellular matrix (ECM)–related molecules. Protein–protein interaction networks were examined using the STRING database (version 11.0) in Cytoscape (version 3.8.0).[19] Interactions were acquired using the following thresholds: confidence interaction scores ≥0.4, active interaction sources=text mining, experiments, databases, coexpression, neighborhood, gene fusion, co-occurrence.

scRNAseq data analyses were performed with R (version 4.1.0).[17] The Seurat package was used to identify cell types.[20] Two Seurat objects for each of the mapped unique molecular identifier count datasets from mGFP-positive cells (control–SHF and AngII–SHF) were built using the CreateSeuratObject function with the following criteria: ≥3 cells and ≥200 detected genes. Cells expressing <200 or >5000 genes were filtered out for exclusion of noncell and cell aggregates, respectively. Cells with >10% mitochondrial genes were also excluded. Each of the unique molecular identifier counts was then normalized as follows: counts for each cell were divided by total counts, multiplied by 10 000, and transformed to natural log. FindIntegrationAnchors and IntegrateData functions were used to remove batch effects and integrate the 2 normalized unique molecular identifier count datasets. Uniform manifold approximation and projection dimensionality reduction to 20 dimensions for the first 30 principal components with 0.1 or 0.5 resolution was applied to identify cell clusters using the normalized and scaled unique molecular identifier count data. FindAllMarkers and FindConcervedMarkers functions were used to identify conserved marker genes to determine cell types of each of the clusters. Differences in cellular proportions between infusions were examined by the χ^2 test. Using zinbwave (1.14.1) and edgeR (3.34.0) R packages,[21,22] differentially expressed genes (DEGs) were identified with a 0-inflated negative binomial regression model using Q<0.05 as a threshold. Gene Ontology enrichment analyses in scRNAseq were performed using clusterProfiler (4.0.2) in genes with Q<0.05 and $|\log_2$fold change$|>0.5$. The monocle package was used for trajectory pseudotime analysis.[23]

Cell–cell interaction was evaluated using a list containing 2009 ligand–receptor pairs developed by Skelly et al.[24] The presence of ligand–receptor pairs within and between each cell type was defined if >20% of cells in that cell type had nonzero read counts for the gene-encoding ligand or receptor. Then 2 cell types were linked and network plots were generated using the igraph package in R.[25]

For human scRNAseq analyses, read count data were downloaded from Gene Expression Omnibus (GSE155468).[26] TAA samples were harvested from the ascending aortic region from patients who underwent surgery for aortic replacement (n=8; mean age, 56–78 years; 4 male, 4 female; mean aortic diameter 4.9–5.8 cm) and control samples were obtained from recipients of heart transplants or lung donors (n=3; mean age, 61–63 years; 1 male, 2 female). mRNA abundance was evaluated in SMC and fibroblast clusters. DEG analyses in SMCs and fibroblasts were performed in R using the Hurdle model adjusted for age implemented in the MAST R package.[27]

RESULTS

Medial Gradients of Aortic Pathologies in Patients With TAAs and AngII-Infused Mice

We first performed histologic analyses to determine the pathologic patterns in human sporadic TAA tissues. Immunostaining for α–smooth muscle actin and Movat pentachrome staining were performed to detect SMCs and ECM, respectively. Immunostaining for α–smooth muscle actin revealed that the outer media had significantly lower positive areas for α–smooth muscle actin than the inner media in human TAA tissues (Figure 1A). Movat pentachrome staining identified higher collagen deposition in the outer media (Figure 1B).

A cell lineage study was performed to investigate the interaction of SMC origins with medial pathologies. CNC- and SHF-derived cells were tracked using Wnt1- or Mef2c-*Cre* ROSA26R^{LacZ} mice infused with AngII, respectively. Consistent with our previous study,[13] the ascending aorta was composed of both CNC- and SHF-derived SMCs (Figure 1C). SHF-derived cells were restricted to the ascending aorta, whereas CNC-derived cells extended into the aortic arch. Although not altering distribution of cells of SMC origins (Figure 1D and 1E), AngII increased medial area (Figure 1F). X-gal–positive areas were increased significantly in medial SHF-derived but not CNC-derived cells (Figure 1G). Because selected adventitial fibroblasts are derived from the SHF,[13] we also evaluated the effects of AngII infusion on cells in the adventitia. Similar to the media, the adventitial area was also increased by AngII infusion (Figure 1H) and increased X-gal–positive areas were observed in SHF-derived but not CNC-derived cells (Figure 1I). Thus, TAAs have a transmural gradient of aortic pathologies in humans and mice. The linear tracing data support the notion that SHF-derived cells are susceptible to AngII-induced outer medial and adventitial thickenings.

AngII Altered Aortic Protein Profiles Related to ECM Organization

To uncover the molecular mechanisms of AngII-induced ascending aortic pathologies, we performed mass spectrometry–assisted proteomics of the ascending aorta of AngII-infused mice. Ascending aortic tissues were harvested at day 3 of either saline or AngII infusion. Aortic samples showing intramural hemorrhage or dissection were excluded. Proteomic analysis identified 2644 proteins among all aortic samples. In principal component analysis using the unfiltered proteome, AngII infusion altered protein profiles significantly (45% variation along principal component 1; Figure 2A). Compared with saline infusion, AngII infusion changed 596 protein abundances (384 and 212 proteins upregulated and downregulated, respectively; Figure 2B). Gene Ontology and Kyoto Encyclopedia of Genes and Genomes pathway enrichment analyses were also performed using these differentially expressed proteins. In addition to terms related to translation and ribosome, ECM-related terms, such as "extracellular matrix organization" and "proteoglycan in cancer," were identified in both Gene Ontology and Kyoto Encyclopedia of Genes and Genomes analyses (Figure 2C and Figure S1A). A protein–protein interaction analysis also demonstrated the presence of ECM-related molecules in the differentially expressed proteins (Figure S1B). Therefore, we assessed ECM-related molecules comprehensively (Figure 2D). Several contractile proteins, including Myh11, were downregulated by AngII, whereas Mmp2 (matrix metalloproteinase 2) was upregulated in AngII-infused mouse aortas. In TGF-β signaling molecules, AngII upregulated Ltbp2 (latent TGF-β binding protein 2) and Tgfb2 (TGF-β2). AngII also increased several ECM components: Col3a1 (collagen type III alpha 1 chain), Col5a2 (collagen type V α2 chain), and Eln (elastin). Other ECM-related molecules—Thbs1 (thrombospondin 1), Fn1 (fibronectin 1) and Tnc (tenascin C)—were also upregulated by AngII infusion. During the short interval of 3 days of infusion, AngII changed the ECM-related proteome significantly in the ascending aorta.

LRP1 is a multifunctional protein that plays a role in ECM maturation.[28] LRP1 deletion in pan-SMCs causes aortic pathologies including aneurysm and tortuosity with ECM degradation.[29–32] Thus, we examined protein abundances of LRP1 and its ligands. Aortic LRP1 protein abundance was not changed by AngII infusion (data not shown, P=0.89); however, multiple LRP1 ligands, including Serpine1 (PAI1 [plasminogen activator inhibitor 1]), were increased by AngII (Figure 2E). A volcano plot demonstrated that Serpine1 was the most significantly increased molecule by AngII infusion (Figure 2B). Because these ligands are internalized into the cytosol through LRP1 for their degradation,[28] these data suggest impairment of aortic LRP1 function. Taken together, these data indicate that the aortic proteome related to ECM was altered as early as day 3 by AngII infusion with the increase of multiple LRP1 ligands.

LRP1 Deletion in SHF-Derived Cells Augmented AngII-Induced Thoracic Aortopathies

Our proteomic analysis, in combination with our previous findings that deletion of LRP1 in pan-SMCs augmented TAA formation with ECM degradation in AngII-infused mice,[30] prompted us to examine whether LRP1 deletion in SHF lineage affects AngII-induced TAA formation. LRP1 was deleted in SHF-derived cells using a Mef2c promoter–driven *Cre*. In Mef2c-*Cre*–expressing mice, *Cre* activity was observed mainly in the outer media (Figure S2A), and the *Lrp1 delta flox* polymerase chain reaction fragment was detected in addition to a band of native *Lrp1* (Figure S2B–S2D),

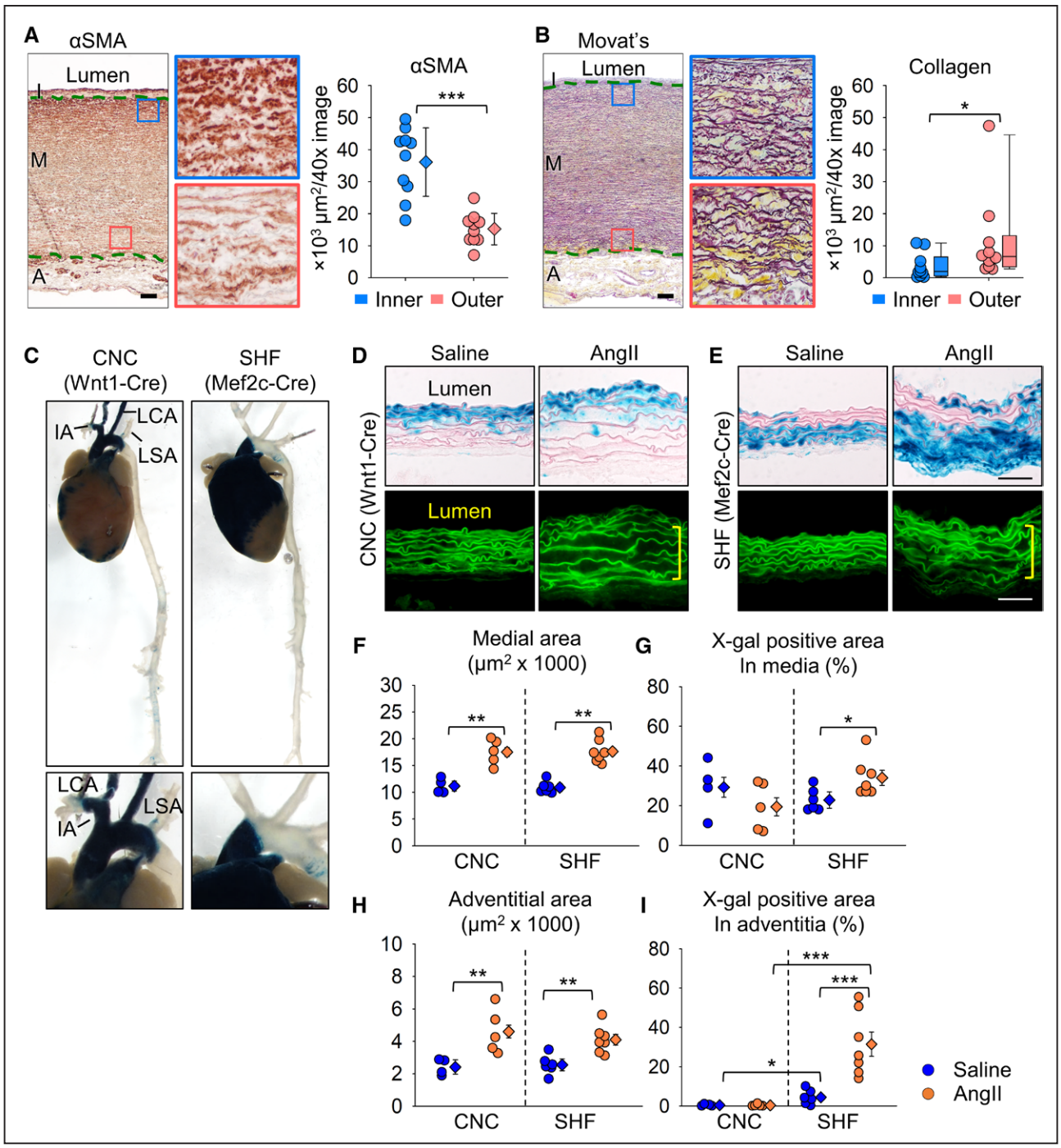

Figure 1. Transmural gradients of aortic pathologies in patients with sporadic thoracic aortic aneurysm and angiotensin II–infused mice.

Representative images of (**A**) immunostaining for α–smooth muscle actin (αSMA; red) and (**B**) Movat pentachrome staining (elastin: dark purple; collagen: yellow). High magnification images are captured from the inner (blue box) and outer (red box) media (n=10). Green dotted lines indicate internal and external elastic layers. αSMA-positive and collagen-deposited areas were quantified in inner and outer media. Log transformation was applied for the data of collagen deposition. **C**, Representative images of X-gal–stained (blue) aortas from Wnt1-*Cre* and Mef2c-*Cre* ROSA26R^{LacZ} mice. High-magnification images of the proximal thoracic aortas. Representative X-gal staining and fluorescein isothiocyanate images of aortas from saline- or AngII-infused (**D**) Wnt1-*Cre* and (**E**) Mef2c-*Cre* ROSA26R^{LacZ} mice (n=5–7 per group). Yellow square brackets indicate medial thickening. Scale bar, 50 μm. Dot plots for (**F**) medial and (**H**) adventitial areas and X-gal–positive area in the (**G**) media and (**I**) adventitia. Diamonds and error bars indicate the mean and SEM, respectively. *P<0.05, **P<0.01, ***P<0.001 by Student t test or 2-way analysis of variance followed by Holm-Sidak test. A indicates adventitia; AngII, angiotensin II; CNC, cardiac neural crest; I, intima; IA, innominate artery; LCA, left common carotid artery; LSA, left subclavian artery; M, media; and SHF, second heart field.

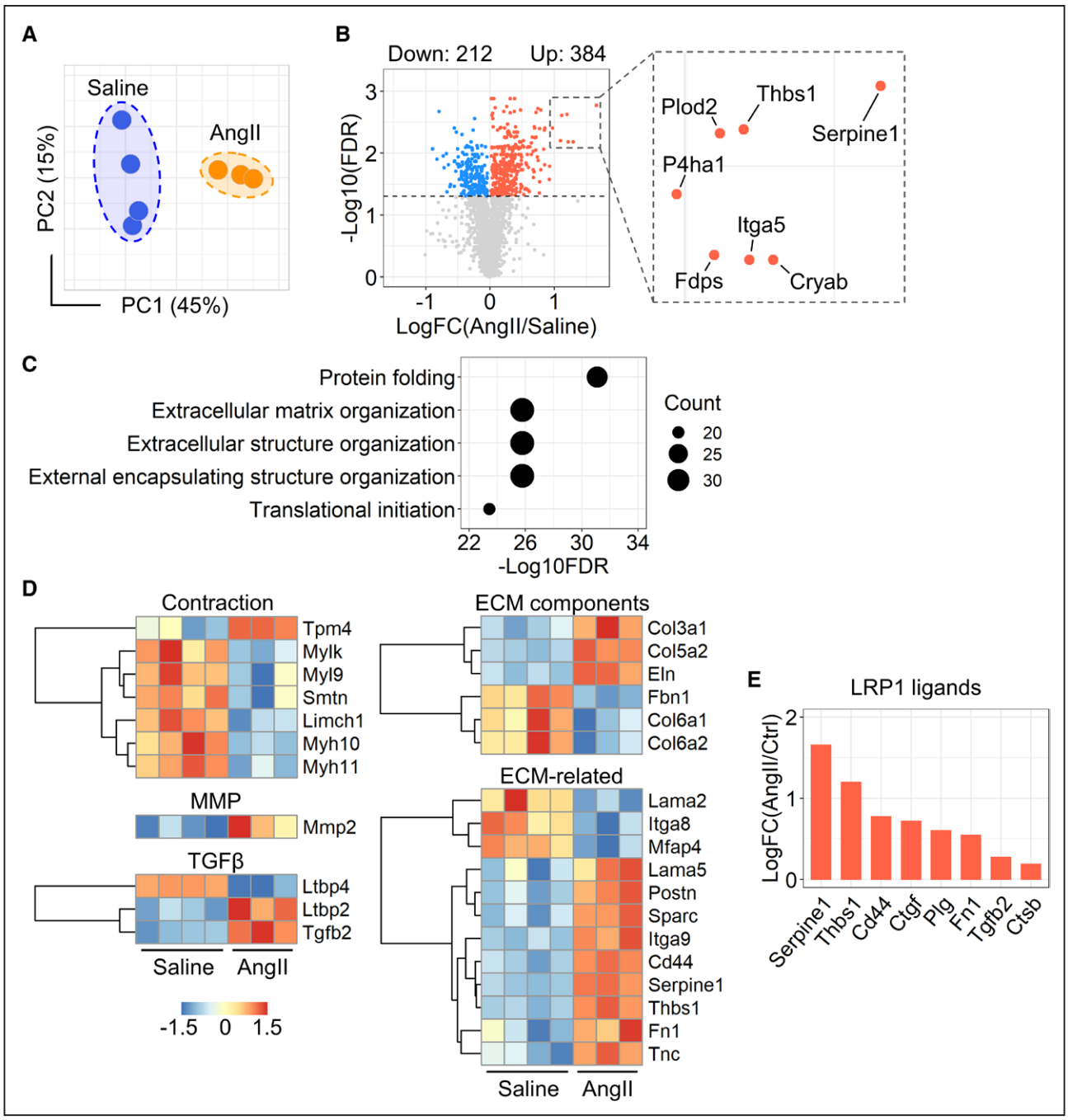

Figure 2. Angiotensin II–altered proteins related to extracellular matrix in the ascending aorta of mice.
A, Principal component (PC) analysis of the unfiltered proteome. PC1/PC2 indicates first/second PCs (n=3 or 4 per group). **B**, Volcano plot for differentiated proteins between ascending aortas of saline- and angiotensin II (AngII)–infused mice. **C**, Top 5 annotations of enrichment analyses in the Gene Ontology biological process. **D**, Heatmap with Z score coloring for proteins related to smooth muscle cell contraction, matrix metalloproteinase (MMP), transforming growth factor–β (TGFβ) signaling, and extracellular matrix (ECM)–related molecules compared between saline and AngII infusion. **E**, Log fold change of LRP1 (low-density lipoprotein receptor–related protein 1) ligands.

confirming DNA recombination of LRP1 in SHF-derived cells. LRP1 protein abundance was reduced by 37% in the ascending aortic media of SHF-specific LRP1-deleted mice compared with *Cre*-negative littermates with LRP1 deletion restricted to the outer media of the ascending aorta (Figure S2E and S2F). Mass spectrometry–assisted proteomics also verified reduction of LRP1 peptide intensity in the ascending aorta of Mef2c-*Cre*–expressing mice (Figure S2G).

SHF-specific LRP1 deletion did not affect growth or development of mice. To promote TAAs, AngII was infused subcutaneously into mice for 4 weeks. LRP1 deletion in SHF-derived cells augmented AngII-induced aortic dilation in the ascending aorta as demonstrated by

both ultrasound and in situ imaging (Figure 3A and 3B). SHF-specific LRP1 deletion also exacerbated AngII-induced ascending aortic rupture and elastin fragmentation (Figure 3C–3E). Systolic blood pressure was not different between genotypes in response to AngII infusion (Figure 3F), demonstrating that augmented aortopathy was independent of systolic blood pressure. These data support that SHF-derived cells exert a critical role in the structural integrity of the ascending aorta.

AngII Infusion Compromised TGF-β Signaling in SHF-Derived SMCs and Fibroblasts

Because using tissues of fate mapping mice enables unbiased transcriptomics profiling in a lineage-specific manner, we investigated molecular roles of SHF-derived cells in AngII-induced TAA formation by scRNAseq in aortas from Mef2c-*Cre* ROSA26R$^{mT/mG}$ mice. Aortic tissues were harvested from Mef2c-*Cre* ROSA26R$^{mT/mG}$ male mice at baseline and after 3 days of AngII infusion. Four to five aortic tissues were pooled to obtain sufficient numbers of aortic cells (Figure 4A). Because mGFP protein was present on Mef2c-*Cre*–expressing cells of this mouse strain, mGFP-positive cells were derived from the SHF (Figure 4B). After sorting cells on the basis of mGFP signal, scRNAseq was performed using mGFP-positive cells.

The 2 normalized datasets were properly integrated (Figure 4C). scRNAseq analysis revealed multiple cell types, including SMC, fibroblast, and endothelial cells, in the mGFP cell population (Figure 4C and 4D and Figure S3A and S3B). At baseline, SHF-derived SMCs were composed of 33% SHF-derived cells, which increased to 55% by AngII infusion (Figure 4D). Meanwhile, fibroblast population declined from 66% to 44%. Because SMCs and fibroblasts comprised the majority of cells, DEG analysis was performed in these clusters. AngII altered 3848 (1862 upregulated, 1986 downregulated) and 3398 (1931 upregulated, 1467 downregulated) genes in SMCs and fibroblasts, respectively (Figures S4A and S5A). Although the top 10 upregulated and downregulated genes were variable between SMCs and fibroblasts, except for *Ptrf* (Figures S4B and S5B), enrichment analysis identified extracellular matrix organization as a common term in SMC and fibroblast clusters (Figures S4C and S5C). Therefore, similar to the proteomic analyses, we next examined ECM-related molecules in the scRNAseq data (Figure 4E and 4F). In

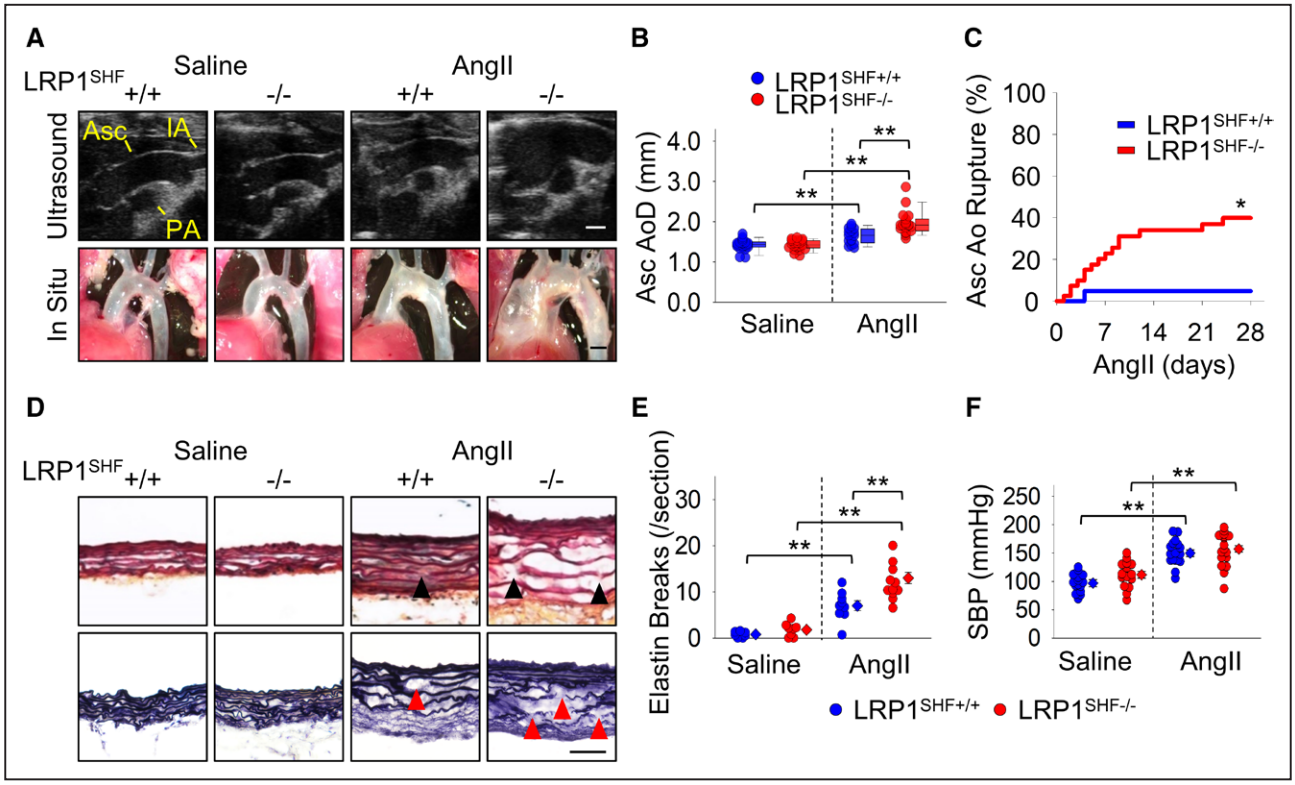

Figure 3. LRP1 deletion in second heart field–derived cells augmented angiotensin II–induced thoracic aortic aneurysm formation and aortic rupture in mice.

A, Representative ultrasound images and in situ gross appearances of proximal thoracic aortas (n=21–40 per group). Scale bar, 1 mm. **B**, Ascending aortic diameter (Asc AoD) measured by ultrasonography. **C**, Cumulative incidence of ascending aortic (Asc Ao) rupture. **D**, Representative Movat and Verhoeff iron hematoxylin staining. Scale bar, 50 μm. Arrowheads indicate elastin fragmentation. **E**, Elastin break counts in Movat-stained sections. **F**, Systolic blood pressure (SBP). Diamonds and error bars indicate the mean and SEM, respectively. *P<0.01 by log-rank test, **P<0.001 by 2-way analysis of variance followed by Holm-Sidak test. Log transformation was applied for the data of ascending aortic diameters. AngII indicates angiotensin II; IA, innominate artery; LRP1, low-density lipoprotein receptor–related protein 1; and PA, pulmonary artery.

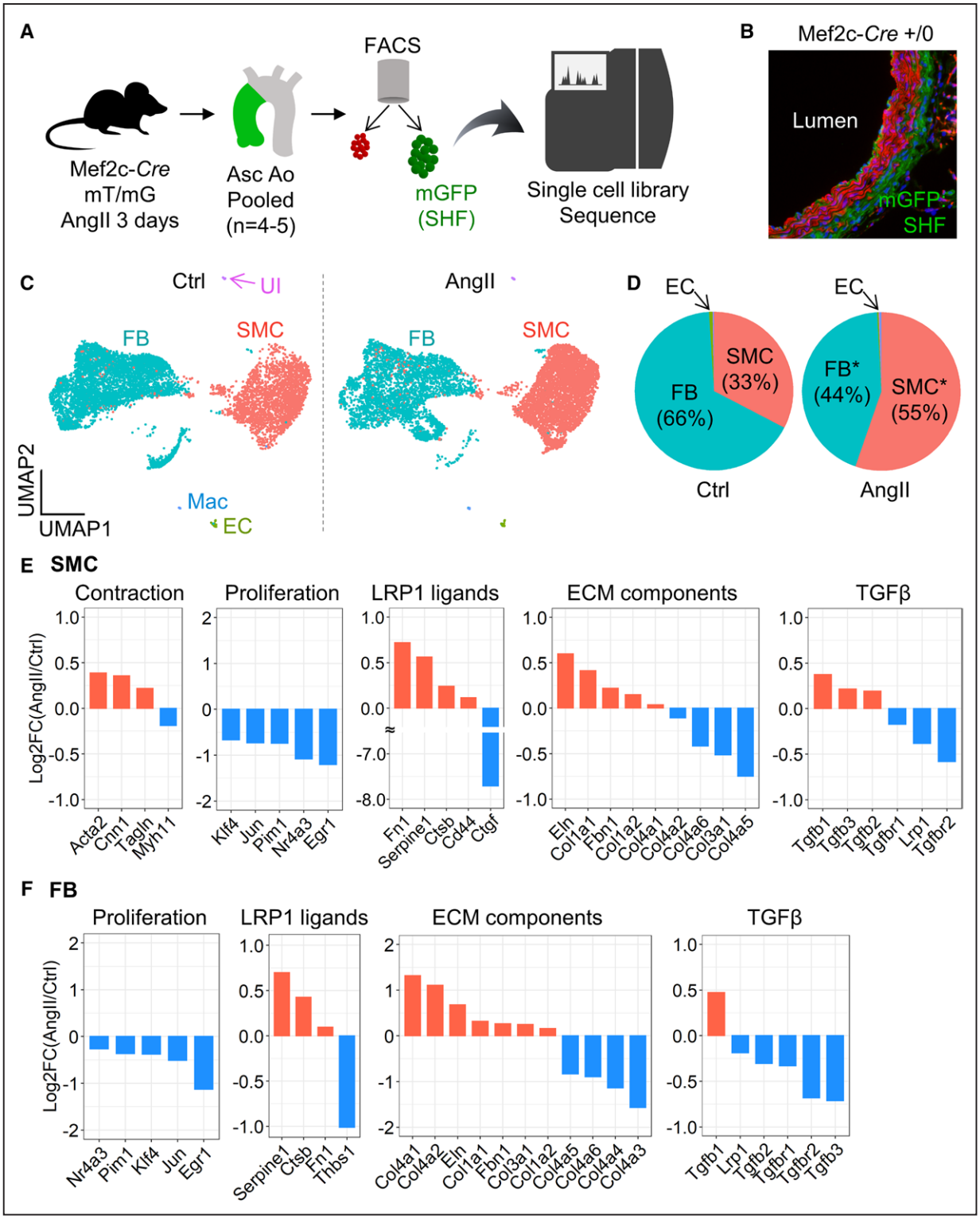

Figure 4. Significant reduction of *Tgfbr2* mRNA in second heart field–derived smooth muscle cells and fibroblasts of angiotensin II–infused mice.

A, Experimental design of single-cell RNA sequencing using Mef2c-*Cre* +/0 ROSA26R$^{mT/mG}$ mice. **B**, Representative fluorescent image of the ascending aorta from Mef2c-*Cre* +/0 ROSA26R$^{mT/mG}$ mice. **C**, Uniform manifold approximation and projection (UMAP) plots of aortic cells at baseline (Ctrl) and after 3 days of angiotensin II (AngII) infusion. **D**, Pie charts for the composition of each cell type. *P<0.0001 by χ^2 test. Log_2 fold change of mRNA abundance related to smooth muscle cell (SMC) contraction, cell proliferation, LRP1 (low-density lipoprotein receptor–related protein 1) ligands, extracellular matrix (ECM) components, and transforming growth factor–β (TGF-β) ligands and receptors between control and AngII in (**E**) SMCs and (**F**) fibroblast (FB) clusters. Asc Ao indicates ascending aorta; EC, endothelial cells; FACS, fluorescence-activated cell sorting; Mac, macrophages; SHF, second heart field; and UI, unidentified cells.

SMCs, *Acta2*, *Cnn1*, and *Tagln*, contractile genes, were increased after 3 days of AngII infusion. Proliferation genes, such as *Klf4* and *Egr1*, were downregulated in both SMCs and fibroblasts by AngII infusion. LRP1 ligands *Serpine1*, *Ctsb* (cathepsin B), and *Fn1* were increased by AngII in SHF-derived SMCs and fibroblasts. Multiple ECM components (*Eln*, *Col1a1*, *Col1a2*, and *Col4a1*) were increased in both SMC and fibroblast clusters in response to AngII infusion. However, TGF-β ligands demonstrated variable responses to AngII between cell types. AngII increased *Tgfb1-3* in SMCs, but *Tgfb2-3* were decreased in fibroblasts. TGF-β receptors, including *Lrp1* and *Tgfbr2*, were significantly downregulated by AngII in both SMCs and fibroblasts.

mRNA abundance of TGF-β ligands and receptors was also examined in human scRNAseq data (GSE155468).[26] SMCs and fibroblasts were extracted and mRNA abundance of *TGFB1-3*, *TGFBR1-2*, and *LRP1* were compared between control and TAA samples. In SMCs, TGF-β ligands and receptors, including *LRP1*, were decreased modestly in TAAs compared with control aortas (Figure S6A). In contrast, TGF-β ligands and receptors were increased in fibroblasts of TAAs, except for *TGFB1* (Figure S6B).

Unique Subcluster of SHF-Derived Fibroblasts in Ascending Aortas of AngII-Infused Mice

Because the aortic wall comprises mostly SMCs and fibroblasts (Figure 4C and 4D), we performed further subclustering analyses in SHF-derived SMCs and fibroblasts. SHF-derived SMCs had 3 distinct clusters, but there was no remarkable alteration during AngII infusion in transcriptomic distributions of these cells (Figure S7). Meanwhile, a unique subcluster (FB4) was observed in SHF-derived fibroblasts of AngII-infused mice (Figure 5A). The FB4 subcluster was composed of 10 and 544 cells at baseline and after 3 days of AngII infusion, respectively (Figure S8A). AngII infusion altered 586 genes in the FB4 subcluster and these genes were significantly associated with cytokinesis, as identified by Gene Ontology analysis (Figure S8B and 8C). To further characterize the FB4 subcluster, featured genes were determined by comparing the transcriptomes among all fibroblast subclusters. Genes related to cell division, such as *H2afz*, *Cks2*, *Cenpa*, *Cdk1*, and *Mki67*, were identified uniquely in the FB4 subcluster (Figure 5B and Figure S9). These results indicate that FB4 cells had enhanced proliferative features. However, FB4 cells were not abundant for *Ly6a*, a marker for Sca1+ fibroblasts (Figure 5C). Whereas the transcriptome of FB4 differed from other fibroblast subclusters (Figure 5D), the ligand–receptor interaction analyses in SMC and fibroblast clusters demonstrated accelerated cell–cell interactions among cell types by AngII infusion (Figure 5E). In particular, the FB4 subcluster had more apparent interactions with SMC and FB1 clusters under AngII infusion. Trajectory analysis demonstrated that FB4 cells were derived from FB1 cells in a pseudotime (Figure 5F). Because of these interactions, we subsequently compared DEGs related to ECM maturation between FB1 and FB4 subclusters (Figure 5G). LRP1 ligands, including *Serpine1*, were all downregulated in FB4. ECM component genes, such as *Eln* and *Col1a1*, were also lower in FB4. TGF-β receptors were further downregulated in FB4 by AngII infusion. Alongside the scRNAseq analyses in SMCs and fibroblasts, these data suggest that AngII compromises the TGF-β signaling pathway in SHF-derived cells, which may contribute to the susceptibility of SHF-derived cells to vascular pathologies.

To investigate the effect of the TGF-β signaling pathway in SHF-derived cells on vascular integrity, we deleted TGFBR2 in SHF-derived cells in mice. SHF-specific TGFBR2 deletion led to embryonic lethality with retroperitoneal hemorrhage beginning at E12.5 (Figure 5H). In addition, the outflow tract was dilated significantly in fetuses with SHF-specific TGFBR2 deletion compared with wild-type littermates (Figure 5H and 5I). Thus, TGFBR2 deficiency in SHF-derived cells led to prenatal vasculopathies, suggesting the importance of SHF-derived cells through TGFBR2 for vascular development and maintenance of its integrity.

Transmedial Gradient of PAI1 in Ascending Aortas of AngII-Infused Mice and Sporadic Ascending TAAs in Humans

We integrated DEG results of proteomics and scRNAseq data from mice. There were 412 overlapped genes between proteomics and scRNAseq using the SHF-SMC cluster and 198 molecules were upregulated in both datasets (highlighted in red; Figure 6A). In SHF fibroblasts, 375 genes were overlapped, and 205 genes were increased (Figure 6B). LRP1 ligands Serpine1, Fn1, and Ctsb were of consistently greater abundance in AngII-infused mice, as shown in proteomics and scRNAseq analyses of SMCs and fibroblasts (Figure 6A and 6B). In protein analyses, PAI1 (*Serpine1*) was the most significantly increased molecule by AngII (Figure 6A and 6B). Western blot analysis showed a striking increase (≈26-fold) of PAI1 in ascending aortas from mice infused with AngII (Figure 6C). Immunostaining of PAI1 was barely detected in aortas from control mice, whereas it was intense in ascending aortas of AngII-infused mice (Figure 6D). In ascending aortas of AngII-infused mice, PAI1 was present through the aortic wall; aortic PAI1 was dominant in the outer media and the adventitia, coincident with the gradient of medial pathologies (Figure 6D).

For clinical relevance, we evaluated *SERPINE1* mRNA abundance and protein distribution in human aortic samples. In the human scRNAseq data (GSE155468),[26] *SERPINE1* abundance was assessed

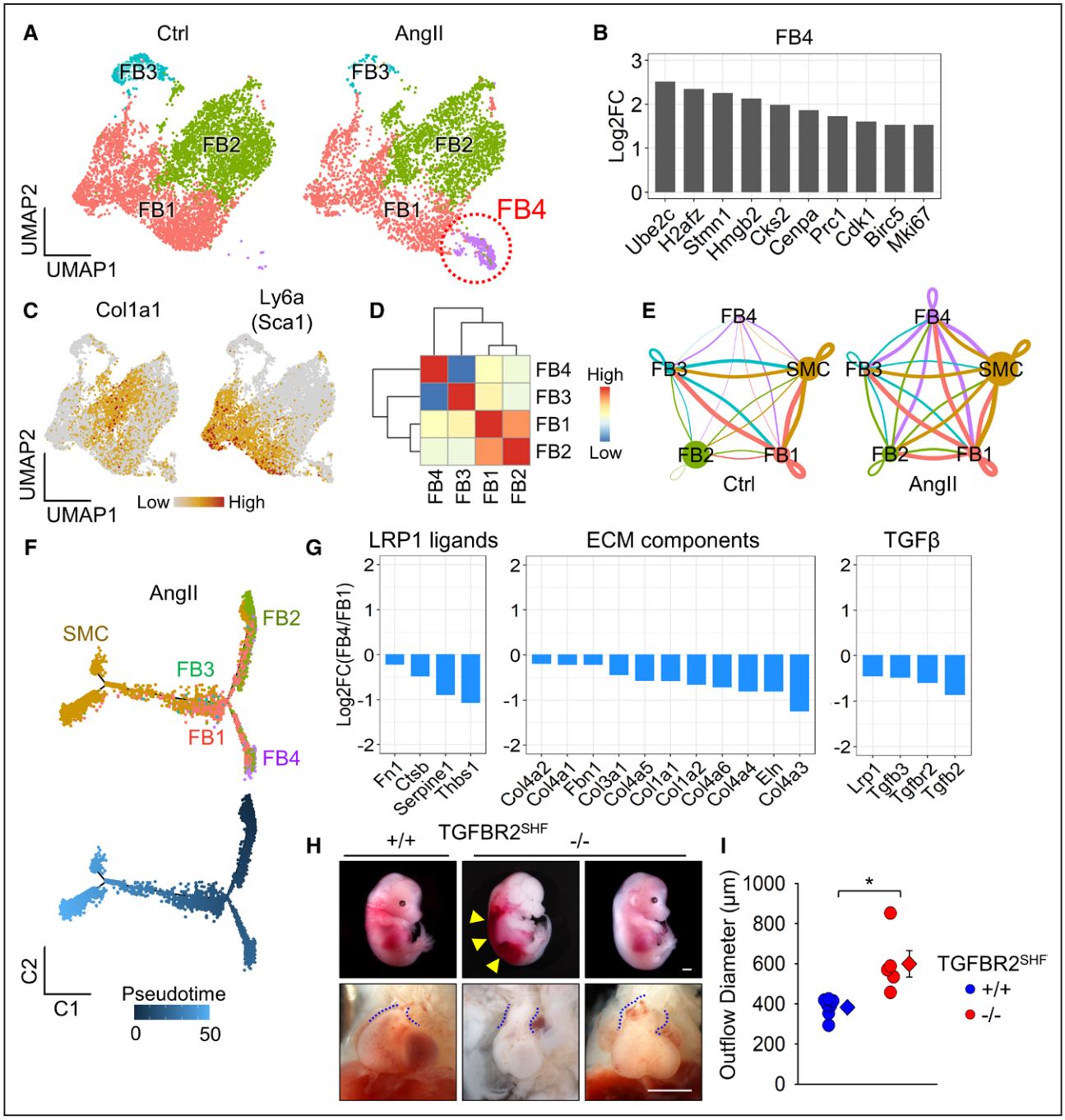

Figure 5. Distinct subcluster with decreased *Tgfbr2* mRNA in second heart field–derived fibroblasts of angiotensin II–infused mice.

A, Uniform manifold approximation and projection (UMAP) plots at baseline (Ctrl) and after 3 days of angiotensin II (AngII) infusion in second heart field (SHF)–derived fibroblasts (FBs). **B**, Log_2 fold change of mRNA abundance for the top 10 unique genes in the FB4 subcluster. **C**, Featured plots for *Col1a1* and *Ly6a* in FB subclusters. **D**, Heatmap for cluster similarity among FB subclusters. **E**, Ligand–receptor interactions among aortic cells. Lines connect to cell populations that express cognate ligands or receptors. The line thickness and node size correspond to the number of cognate ligand–receptor expression and cell number, respectively. **F**, Trajectory analysis in smooth muscle cell (SMC) and FB subclusters from AngII-infused mice. **G**, Log_2 fold change of mRNA abundance related to LRP1 (low-density lipoprotein receptor–related protein 1) ligands, extracellular matrix (ECM) components, and transforming growth factor–β (TGF-β) molecules between FB1 and FB4 subclusters after AngII infusion. **H**, Representative images of gross appearance and the outflow tract of wild-type littermates (**left**), dead (**middle**), and survived (**right**) fetuses with SHF-specific TGFBR2 (transforming growth factor–β receptor type 2) deletion at E12.5. Blue dotted lines indicate the edge of the outflow tract. Yellow triangles indicate retroperitoneal hemorrhage. **I**, Outflow diameter was measured at 300 to 400 μm distal to the root of viable fetuses at termination (n=5–7 per group). Scale bar, 1 mm. Diamonds and error bars indicate the mean and SEM, respectively. *$P<0.001$ by 2-tailed Student *t* test.

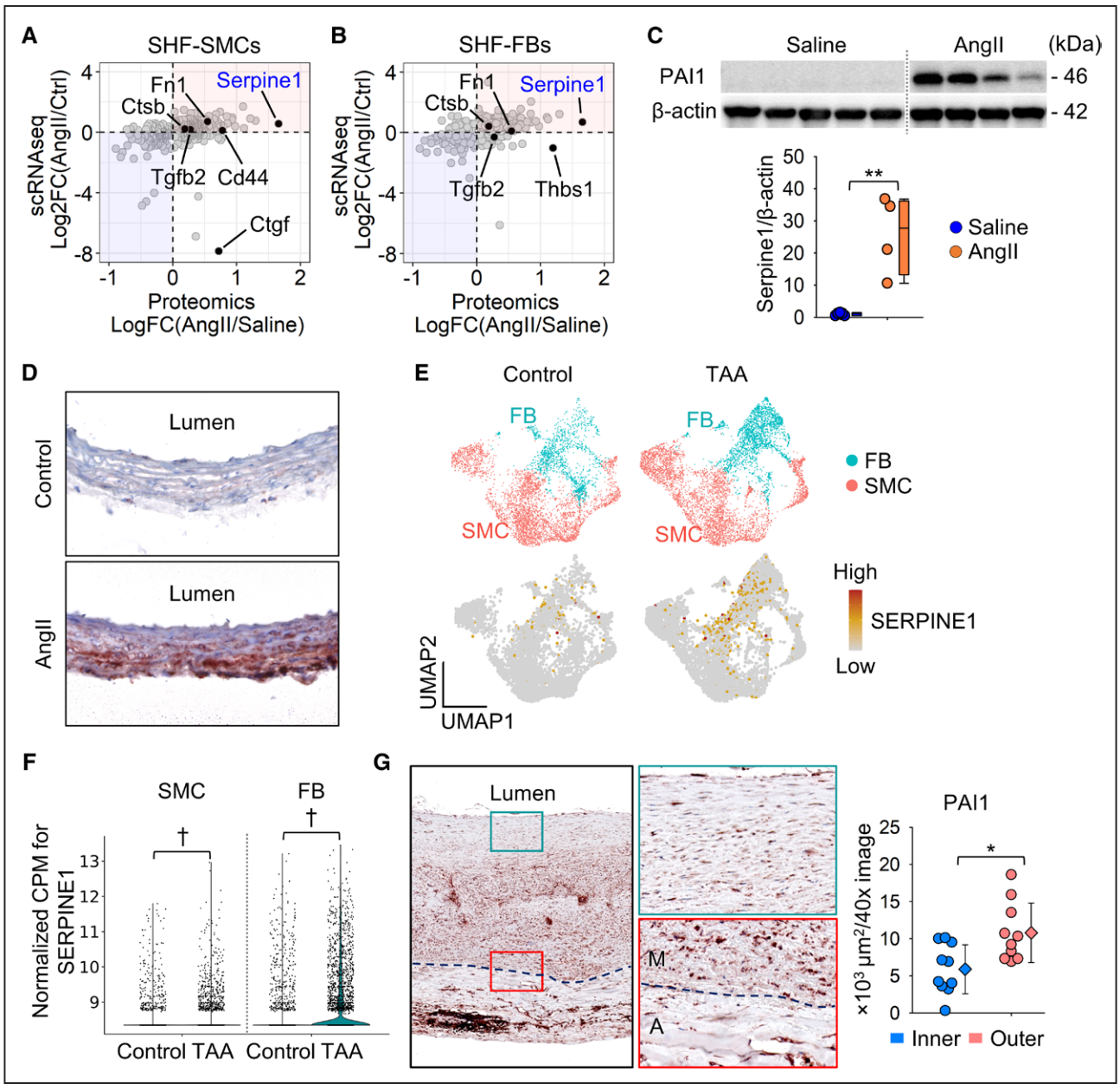

Figure 6. Integration of proteomic and scRNAseq results identified PAI1 (Serpine1) as a key contributor to the medial gradient of aortic pathologies.

Scatter plots for log or $\log_2$ fold change of protein and mRNA abundances. Data were compared between proteomics and single-cell RNA sequencing (scRNAseq) in second heart field (SHF)–derived (**A**) smooth muscle cell (SMC) and (**B**) fibroblast (FB) clusters. Selected LRP1 (low-density lipoprotein receptor–related protein 1) ligands are highlighted. **C**, Western blot analysis for PAI1 (plasminogen activator inhibitor 1; Serpine1) and β-actin in the whole ascending aorta from saline or angiotensin II (AngII)–infused mice (n=4–5 per group). ***P*<0.001 by Student *t* test after log transformation. **D**, Representative images of immunostaining for PAI1 (red) in ascending aortas from control or AngII-infused mice (n=7 per group). **E**, Uniform manifold approximation and projection (UMAP) and (**F**) violin plots for *SERPINE1* in SMC and FB clusters of controls and patients with ascending thoracic aortic aneurysms (TAAs; n=3 and 8 per group; scRNAseq data were downloaded from GSE155468). †*P*<0.001 analyzed using the Hurdle model adjusted for age implemented. **G**, Representative images of immunostaining for PAI1 in patients with sporadic ascending TAA (n=10) and its quantification. Dotted lines indicate external elastic laminae. Diamonds and error bars indicate the mean and SEM, respectively. **P*<0.01 by Student *t* test. A indicates adventitia; and M, media.

in SMC and fibroblast clusters. Uniform manifold approximation and projection plots showed the presence of *SERPINE1* in both SMC and fibroblast clusters of control and TAA samples (Figure 6E); *SERPINE1* was significantly higher in SMCs and fibroblasts of human TAA samples compared with controls (Figure 6F). Immunostaining demonstrated that PAI1 was expressed in the aortic media and adventitia of human TAA samples (Figure 6G). Consistent with AngII-infused mouse aortas (Figure 6D), highly abundant areas of PAI1 were observed in the outer media adjacent to the external elastic lamina in most TAA tissues (Figure 6G).

DISCUSSION

Our study demonstrated that (1) aortic pathologies were mainly observed in the outer media of the ascending aorta in patients with TAAs and AngII-infused mice, (2) SHF-derived cells were responsible for AngII-induced medial and adventitial thickening in the ascending aorta, (3) AngII altered protein profiles related to ECM and LRP1 ligands, (4) AngII decreased *Tgfbr2* mRNA in SHF-derived SMCs and fibroblasts, (5) AngII led to a distinct subcluster of SHF-derived fibroblasts that had lower *Tgfbr2* mRNA abundance, (6) either LRP1 or TGFBR2 deletion in SHF-derived cells led to vasculopathies in mice, and (7) proteomic and scRNAseq analyses identified PAI1 as a key molecule that showed a transmedial gradient in the ascending aorta of AngII-infused mice or human TAA tissues. This study provides compelling evidence to support the importance of SHF-derived cells in maintaining aortic wall integrity.

A number of studies have shown an important role for TGF-β signaling in maintaining aortic wall integrity.[9,33–35] Both LRP1 and TGFBR2 are related to the TGF-β signaling pathways[28,33] and genetic deletions of these molecules in pan-SMCs promote TAA formation in mice.[8,9,29–31,36] Therefore, in the current study, the biological effects of SHF-derived cells in aortic integrity were investigated by SHF-specific deletion of either LRP1 or TGFBR2. SHF-specific TGFBR2 deletion led to vascular malformation and SHF-specific LRP1 deletion recapitulated aortic phenotypes in mice with its deletion in pan-SMCs. Thus, we concluded that SHF-derived cells were functionally important in maintenance of vascular wall structural integrity.

The current study revealed that deletion of either TGFBR2 or LRP1 in SHF-derived cells promotes vasculopathies. These data are consistent with the outer layers of SMC-derived cells being crucial for development of vascular pathologies related to TGF-β signaling. A previous study using mice expressing a fibrillin-1 mutation (*Fbn1*$^{C1041G/+}$) reported that heterozygous deletion of *Notch1* in SHF-derived cells had a trend for augmenting luminal dilatation of the aortic sinus.[37] In contrast, another study demonstrated that Smad2 deletion in CNC-derived cells reduced dilation of the aortic sinus in a mouse model of Loeys-Dietz syndrome.[38] Because there are aortic region-specific responses to TGF-β,[39] these 2 developmental origins may have divergent pathophysiologic functions in different aortic regions.

Elastin fragmentation is a pathologic feature of TAAs and is associated with decrease in aortic resilience.[40,41] Elastic fibers are one of the major matrix components and are vital for maintaining aortic structure.[42] Mutations of the elastin gene cause aortic stenosis attributable to overgrowth of SMCs.[40,41] SMC-specific elastin deletion induces aortic extension and coarctation in mice.[43] Our proteomic and scRNAseq analyses demonstrated increased aortic elastin in response to AngII infusion. These data suggest that de novo elastin synthesis is a compensatory reaction for maintaining aortic integrity during AngII stimulation. Major TGF-β receptors, *Tgfbr2* and *Lrp1*, were downregulated during AngII infusion for 3 days in SHF-derived SMCs and fibroblasts, although the TGF-β signaling pathway plays an important role in ECM maturation.[44] Hence, increase of aortic elastin in SHF-derived cells may not be regulated through the TGF-β signaling pathway directly during this interval. In addition, multiple collagen genes showed variable responses to AngII infusion. Therefore, it remains to be clarified which ECM component molecules are regulated during AngII infusion.

Our proteomic and scRNAseq analyses identified PAI1 as a key molecule in AngII-induced TAA formation. PAI1 has been implicated in thoracic aortic diseases by omics approaches in several previous studies.[45,46] A microarray of aortas from patients with aortic dissections revealed an increase of PAI1 mRNA abundance in dissected aortas.[45] scRNAseq using aortas from patients with Marfan syndrome and a mouse model of this disease demonstrated the presence of PAI1 in aortic SMCs.[46] Consistent with these reports, the current study also identified PAI1 in the ascending aorta shortly after initiation of AngII infusion. Aortic PAI1 was increased dramatically by AngII. Furthermore, our histologic analyses found a transmedial gradient of PAI1 in AngII-infused mice and human TAA samples. The distinct distribution of PAI1 was matched with the medial gradient of aortic pathologies, consistent with PAI1 contributing to the complex mechanism of TAA formation.

Several articles have investigated a role of PAI1 in abdominal aortic aneurysms.[47–49] Focal overexpression of PAI1 inhibited aneurysm formation in the abdominal aorta of a rat model using xenograft.[47] Adventitial overexpression of PAI1 protected against abdominal aneurysm formation in AngII-infused mice.[48] In addition, systemic deletion of PAI1 augmented elastase-induced abdominal aortic aneurysms in mice.[49] Therefore, PAI1 plays a protective role in development of abdominal aortic aneurysms. However, molecular mechanisms underlying TAAs and abdominal aortic aneurysms are distinct. There is a lack of evidence showing biological function of PAI in thoracic aortopathies. PAI1 is a ligand for LRP1 and involved in the TGF-β signaling pathway.[50–52] In subsequent studies, we will elucidate the role of PAI1 in SHF-derived cells on TAA formation as well as TGF-β signaling pathway through LRP1.

SHF-specific TGFBR2 deletion led to dilatation of the outflow tract with postperitoneal hemorrhage. Thus, TGFBR2 in SHF-derived cells is essential for vascular development and integrity. However, because of the embryonic lethality by constitutive deletion of TGFBR2 in SMCs, the role of TGFBR2 in SHF-derived cells on thoracic aortopathies remains unclear. The *Mef2c* gene is not

sufficiently expressed in the cardiovascular system at the postnatal phase, especially in normal conditions during the adult phase.[53] Therefore, it is not feasible to activate Mef2c-*Cre* using the ER^{T2} system in adult mice. Development of research methods is needed to overcome the barrier to postnatal gene manipulation in the SHF origin.

Previous studies have reported that prenatal deletion of TGFBR2 in CNC-derived cells results in cleft palate and a congenital heart defect (persistent truncus arteriosus).[54,55] Therefore, there is compelling evidence that CNC-derived cells exert a pivotal role in the integrity of the cardiovascular system.[54,55] However, the current study focused on the role of SHF-derived cells in thoracic aortopathies, because scRNAseq data revealed the important role of these cells in the regulation of elastin and TGF-β signaling genes. Furthermore, our mouse studies demonstrated vascular phenotypes by gene manipulation in SHF-derived cells. These results support the notion that SHF-derived cells are crucial in maintaining aortic wall integrity. Consistent with this notion, a recent study reported that a *TGFBR1* mutation suppressed muscle contractility in SMCs from the SHF, but not CNC, origin.[56] However, it is desirable to directly compare the role of 2 different SMC origins on formation of thoracic aortopathies.

Our scRNAseq identified a distinct fibroblast subcluster and AngII infusion further decreased *Tgfbr2* mRNA abundance in the distinct fibroblast subcluster compared with other fibroblasts. Because TGFBR2 deletion in SHF-derived cells led to vascular malformation, the reduction of *Tgfbr2* mRNA abundance by AngII in this cluster may exert a deleterious role in the pathophysiology of TAAs. scRNAseq enabled us to evaluate cellular heterogeneity and identify a unique cellular cluster, which is an advantage of scRNAseq. However, it is difficult to investigate cluster-specific molecular mechanisms. A technical breakthrough is needed to manipulate specific subclusters for understanding their role in the pathophysiology of TAAs.

scRNAseq demonstrated that *Tgfbr2* and *Lrp1* were downregulated by AngII infusion in both SMCs and fibroblasts derived from the SHF of mouse aortas. In human aortas, *TGFBR2* and *LRP1* were decreased in SMCs of TAAs, but increased in fibroblasts of TAAs. *TGFBR2* and *LRP1* in fibroblasts in human scRNAseq conflict with the mouse scRNAseq results. In the mouse scRNAseq, aortic samples were harvested at day 3 of AngII infusion before TAA formation, but human scRNAseq used aortas at an advanced stage of disease that were acquired during surgical repair. Because the role of TGF-β signaling changes depending on disease stage,[57] this may contribute to the differences in scRNAseq results seen between humans and mice in the current study. In addition, because it was not feasible to discern embryonic origins in the human scRNAseq dataset, the data were analyzed using all SMCs and fibroblasts rather than isolated SHF-derived cells, which may also contribute to the differences seen in these scRNAseq results.

Our study highlights the functional importance of SHF-derived cells in maintaining vascular integrity using multiple TAA mouse models. This study provides strong evidence that SHF-derived cells exert a role during development of thoracic aortopathies. Heterogeneity of SHF-derived cells contributes to complex mechanisms of aortopathy formation, which should be taken into consideration when investigating the pathogenesis of thoracic aortopathies.

ARTICLE INFORMATION

Received October 29, 2021; accepted January 27, 2022.

Affiliations

Saha Cardiovascular Research Center (H.S., J.Z.C., M.K.F., J.J.M., D.A.H., D.L.R., H.S.L., A.D.), Saha Aortic Center (H.S., H.S.L., A.D.), and Department of Physiology (H.S., J.Z.C., H.S.L., A.D.), College of Medicine, Department of Biostatistics, College of Public Health (Y.K.), and Sanders-Brown Center on Aging (Y.K.), University of Kentucky, Lexington. Center for Interdisciplinary Cardiovascular Sciences, Cardiovascular Division, Department of Medicine, Brigham and Women's Hospital, Harvard Medical School, Boston, MA (H.H., S.M., L.H.L., S.A.S., M.A.). Division of Cardiothoracic Surgery, Michael E. DeBakey Department of Surgery, Baylor College of Medicine, Houston, TX (C.Z., Y.L., Y.H.S., S.A.L.). Department of Cardiovascular Surgery, Texas Heart Institute, Houston (C.Z., Y.L., Y.H.S., S.A.L.). Departments of Laboratory Medicine and Pathology (M.W.M.) and Pediatrics (M.W.M.), University of Washington, Seattle. Center for Developmental Biology & Regenerative Medicine, Seattle Children's Research Institute, WA (M.W.M.).

Acknowledgments

Drs Sawada, Higashi, Zhang, Li, Morgan, Singh, Chen, Shen, Aikawa, Majesky, Lu, and Daugherty and D.L. Rateri contributed to study design. Drs Sawada and Zhang and J.J. Moorleghen, D.A. Howatt, and D.L. Rateri implemented animal experiments. Dr Sawada, M.K. Franklin, D.A. Howatt, and D.L. Rateri performed histologic analyses. Drs Sawada, Katsumata, Lu, and Daugherty and D.L. Rateri performed data analyses. Drs Sawada, Katsumata, Higashi, Morgan, Lee, and Singh performed proteomics and associated informatics. Drs Sawada, Katsumata, Zhang, Li, and Shen performed scRNAseq and associated informatics. Drs Singh, Shen, LeMaire, Aikawa, Majesky, Lu, and Daugherty performed supervision and data verification. Dr Sawada wrote the draft manuscript. All authors contributed to editing the manuscript.

Sources of Funding

The authors' research work was supported by the National Heart, Lung, and Blood Institute of the National Institutes of Health (R01HL133723, R35HL15649 [Dr Daugherty], R01HL126901 [Dr Aikawa], R01HL149302 [Dr Aikawa], R01HL121877 [Dr Majesky]) and the American Heart Association Strategically Focused Research Network in Vascular Disease (18SFRN33960163 and 33960114). Dr Sawada was supported by an American Heart Association postdoctoral fellowship (18POST33990468). Dr Chen was supported by the National Center for Advancing Translational Sciences (UL1TR001998) and the National Heart, Lung, and Blood Institute (F30HL143943). Dr LeMaire is supported in part by the Jimmy and Roberta Howell Professorship in Cardiovascular Surgery at Baylor College of Medicine. The content in this article is solely the responsibility of the authors and does not necessarily represent the official views of the National Institutes of Health.

Disclosures

Dr Higashi is an employee of Kowa Company, Ltd, and was a visiting scientist at Brigham and Women's Hospital when the study was conducted. The other authors report no conflicts.

Supplemental Material

Supplemental Methods
Tables S1–S5
Figures S1–S9
Excel Files S1–S3
References 58–61

REFERENCES

1. Goldfinger JZ, Halperin JL, Marin ML, Stewart AS, Eagle KA, Fuster V. Thoracic aortic aneurysm and dissection. *J Am Coll Cardiol.* 2014;64:1725–1739. doi: 10.1016/j.jacc.2014.08.025
2. Hiratzka LF, Bakris GL, Beckman JA, Bersin RM, Carr VF, Casey DE Jr, Eagle KA, Hermann LK, Isselbacher EM, Kazerooni EA, et al; American College of Cardiology Foundation/American Heart Association Task Force on Practice Guidelines; American Association for Thoracic Surgery; American College of Radiology; American Stroke Association; Society of Cardiovascular Anesthesiologists; Society for Cardiovascular Angiography and Interventions; Society of Interventional Radiology; Society of Thoracic Surgeons; Society for Vascular Medicine. 2010 ACCF/AHA/AATS/ACR/ASA/SCA/SCAI/SIR/STS/SVM guidelines for the diagnosis and management of patients with thoracic aortic disease: a report of the American College of Cardiology Foundation/American Heart Association task force on practice guidelines, American Association for Thoracic Surgery, American College of Radiology, American Stroke Association, Society of Cardiovascular Anesthesiologists, Society for Cardiovascular Angiography and Interventions, Society of Interventional Radiology, Society of Thoracic Surgeons, and Society for Vascular Medicine. *J Am Coll Cardiol.* 2010;55:e27–e129. doi: 10.1016/j.jacc.2010.02.015
3. Isselbacher EM. Thoracic and abdominal aortic aneurysms. *Circulation.* 2005;111:816–828. doi: 10.1161/01.CIR.0000154569.08857.7A
4. Albornoz G, Coady MA, Roberts M, Davies RR, Tranquilli M, Rizzo JA, Elefteriades JA. Familial thoracic aortic aneurysms and dissections: incidence, modes of inheritance, and phenotypic patterns. *Ann Thorac Surg.* 2006;82:1400–1405. doi: 10.1016/j.athoracsur.2006.04.098
5. Trachet B, Piersigilli A, Fraga-Silva RA, Aslanidou L, Sordet-Dessimoz J, Astolfo A, Stampanoni MF, Segers P, Stergiopulos N. Ascending aortic aneurysm in angiotensin II-infused mice: formation, progression, and the role of focal dissections. *Arterioscler Thromb Vasc Biol.* 2016;36:673–681. doi: 10.1161/ATVBAHA.116.307211
6. Daugherty A, Rateri DL, Charo IF, Owens AP, Howatt DA, Cassis LA. Angiotensin II infusion promotes ascending aortic aneurysms: attenuation by CCR2 deficiency in apoE-/- mice. *Clin Sci (Lond).* 2010;118:681–689. doi: 10.1042/CS20090372
7. Wanga S, Hibender S, Ridwan Y, van Roomen C, Vos M, van der Made I, van Vliet N, Franken R, van Riel LA, Groenink M, et al. Aortic microcalcification is associated with elastin fragmentation in Marfan syndrome. *J Pathol.* 2017;243:294–306. doi: 10.1002/path.4949
8. Yang P, Schmit BM, Fu C, DeSart K, Oh SP, Berceli SA, Jiang Z. Smooth muscle cell-specific Tgfbr1 deficiency promotes aortic aneurysm formation by stimulating multiple signaling events. *Sci Rep.* 2016;6:35444. doi: 10.1038/srep35444
9. Li W, Li Q, Jiao Y, Qin L, Ali R, Zhou J, Ferruzzi J, Kim RW, Geirsson A, Dietz HC, et al. Tgfbr2 disruption in postnatal smooth muscle impairs aortic wall homeostasis. *J Clin Invest.* 2014;124:755–767. doi: 10.1172/JCI69942
10. Sawada H, Chen JZ, Wright BC, Sheppard MB, Lu HS, Daugherty A. Heterogeneity of aortic smooth muscle cells: a determinant for regional characteristics of thoracic aortic aneurysms? *J Transl Int Med.* 2018;6:93–96. doi: 10.2478/jtim-2018-0023
11. Quintana RA, Taylor WR. Cellular mechanisms of aortic aneurysm formation. *Circ Res.* 2019;124:607–618. doi: 10.1161/CIRCRESAHA.118.313187
12. Majesky MW. Developmental basis of vascular smooth muscle diversity. *Arterioscler Thromb Vasc Biol.* 2007;27:1248–1258. doi: 10.1161/ATVBAHA.107.141069
13. Sawada H, Rateri DL, Moorleghen JJ, Majesky MW, Daugherty A. Smooth muscle cells derived from second heart field and cardiac neural crest reside in spatially distinct domains in the media of the ascending aorta: brief report. *Arterioscler Thromb Vasc Biol.* 2017;37:1722–1726. doi: 10.1161/ATVBAHA.117.309599
14. Luo W, Wang Y, Zhang L, Ren P, Zhang C, Li Y, Azares AR, Zhang M, Guo J, Ghaghada KB, et al. Critical role of cytosolic DNA and its sensing adaptor STING in aortic degeneration, dissection, and rupture. *Circulation.* 2020;141:42–66. doi: 10.1161/CIRCULATIONAHA.119.041460
15. Robinet P, Milewicz DM, Cassis LA, Leeper NJ, Lu HS, Smith JD. Consideration of sex differences in design and reporting of experimental arterial pathology studies: statement from ATVB council. *Arterioscler Thromb Vasc Biol.* 2018;38:292–303. doi: 10.1161/ATVBAHA.117.309524
16. Lu H, Howatt DA, Balakrishnan A, Moorleghen JJ, Rateri DL, Cassis LA, Daugherty A. Subcutaneous angiotensin II infusion using osmotic pumps induces aortic aneurysms in mice. *J Vis Exp.* 2015:doi: 10.3791/53191.
17. R Foundation for Statistical Computing. R: A language and environment for statistical computing. Published 2021. https://www.R-project.org/
18. Kanehisa M, Goto S. KEGG: Kyoto Encyclopedia of Genes and Genomes. *Nucleic Acids Res.* 2000;28:27–30. doi: 10.1093/nar/28.1.27
19. Szklarczyk D, Gable AL, Lyon D, Junge A, Wyder S, Huerta-Cepas J, Simonovic M, Doncheva NT, Morris JH, Bork P, et al. STRING v11: protein-protein association networks with increased coverage, supporting functional discovery in genome-wide experimental datasets. *Nucleic Acids Res.* 2019;47(D1):D607–D613. doi: 10.1093/nar/gky1131
20. Butler A, Hoffman P, Smibert P, Papalexi E, Satija R. Integrating single-cell transcriptomic data across different conditions, technologies, and species. *Nat Biotechnol.* 2018;36:411–420. doi: 10.1038/nbt.4096
21. Risso D, Perraudeau F, Gribkova S, Dudoit S, Vert JP. A general and flexible method for signal extraction from single-cell RNA-seq data. *Nat Commun.* 2018;9:284. doi: 10.1038/s41467-017-02554-5
22. Robinson MD, McCarthy DJ, Smyth GK. edgeR: a Bioconductor package for differential expression analysis of digital gene expression data. *Bioinformatics.* 2010;26:139–140. doi: 10.1093/bioinformatics/btp616
23. Trapnell C, Cacchiarelli D, Grimsby J, Pokharel P, Li S, Morse M, Lennon NJ, Livak KJ, Mikkelsen TS, Rinn JL. The dynamics and regulators of cell fate decisions are revealed by pseudotemporal ordering of single cells. *Nat Biotechnol.* 2014;32:381–386. doi: 10.1038/nbt.2859
24. Skelly DA, Squiers GT, McLellan MA, Bolisetty MT, Robson P, Rosenthal NA, Pinto AR. Single-cell transcriptional profiling reveals cellular diversity and intercommunication in the mouse heart. *Cell Rep.* 2018;22:600–610. doi: 10.1016/j.celrep.2017.12.072
25. Csárdi G, Nepusz T. The igraph software package for complex network research. *InterJournal Complex Systems.* 2006;1695:1–9.
26. Li Y, Ren P, Dawson A, Vasquez HG, Ageedi W, Zhang C, Luo W, Chen R, Li Y, Kim S, et al. Single-cell transcriptome analysis reveals dynamic cell populations and differential gene expression patterns in control and aneurysmal human aortic tissue. *Circulation.* 2020;142:1374–1388. doi: 10.1161/CIRCULATIONAHA.120.046528
27. Finak G, McDavid A, Yajima M, Deng J, Gersuk V, Shalek AK, Slichter CK, Miller HW, McElrath MJ, Prlic M, et al. MAST: a flexible statistical framework for assessing transcriptional changes and characterizing heterogeneity in single-cell RNA sequencing data. *Genome Biol.* 2015;16:278. doi: 10.1186/s13059-015-0844-5
28. Strickland DK, Au DT, Cunfer P, Muratoglu SC. Low-density lipoprotein receptor-related protein-1: role in the regulation of vascular integrity. *Arterioscler Thromb Vasc Biol.* 2014;34:487–498. doi: 10.1161/ATVBAHA.113.301924
29. Boucher P, Gotthardt M, Li WP, Anderson RG, Herz J. LRP: role in vascular wall integrity and protection from atherosclerosis. *Science.* 2003;300:329–332. doi: 10.1126/science.1082095
30. Davis FM, Rateri DL, Balakrishnan A, Howatt DA, Strickland DK, Muratoglu SC, Haggerty CM, Fornwalt BK, Cassis LA, Daugherty A. Smooth muscle cell deletion of low-density lipoprotein receptor-related protein 1 augments angiotensin II-induced superior mesenteric arterial and ascending aortic aneurysms. *Arterioscler Thromb Vasc Biol.* 2015;35:155–162. doi: 10.1161/ATVBAHA.114.304683
31. Basford JE, Koch S, Anjak A, Singh VP, Krause EG, Robbins N, Weintraub NL, Hui DY, Rubinstein J. Smooth muscle LDL receptor-related protein-1 deletion induces aortic insufficiency and promotes vascular cardiomyopathy in mice. *PLoS One.* 2013;8:e82026. doi: 10.1371/journal.pone.0082026
32. Muratoglu SC, Belgrave S, Hampton B, Migliorini M, Coksaygan T, Chen L, Mikhailenko I, Strickland DK. LRP1 protects the vasculature by regulating levels of connective tissue growth factor and HtrA1. *Arterioscler Thromb Vasc Biol.* 2013;33:2137–2146. doi: 10.1161/ATVBAHA.113.301893
33. Lindsay ME, Dietz HC. Lessons on the pathogenesis of aneurysm from heritable conditions. *Nature.* 2011;473:308–316. doi: 10.1038/nature10145
34. Schmit BM, Yang P, Fu C, DeSart K, Berceli SA, Jiang Z. Hypertension overrides the protective effect of female hormones on the development of aortic aneurysm secondary to Alk5 deficiency via ERK activation. *Am J Physiol Heart Circ Physiol.* 2015;308:H115–H125. doi: 10.1152/ajpheart.00521.2014
35. Gallo EM, Loch DC, Habashi JP, Calderon JF, Chen Y, Bedja D, van Erp C, Gerber EE, Parker SJ, Sauls K, et al. Angiotensin II-dependent TGF-β signaling contributes to Loeys-Dietz syndrome vascular pathogenesis. *J Clin Invest.* 2014;124:448–460. doi: 10.1172/JCI69666
36. Hu JH, Wei H, Jaffe M, Airhart N, Du L, Angelov SN, Yan J, Allen JK, Kang I, Wight TN, et al. Postnatal deletion of the type II transforming growth factor-β receptor in smooth muscle cells causes severe aortopathy in mice. *Arterioscler Thromb Vasc Biol.* 2015;35:2647–2656. doi: 10.1161/ATVBAHA.115.306573
37. Koenig SN, LaHaye S, Feller JD, Rowland P, Hor KN, Trask AJ, Janssen PM, Radtke F, Lilly B, Garg V. Notch1 haploinsufficiency causes as-

cending aortic aneurysms in mice. *JCI Insight.* 2017;2:91353. doi: 10.1172/jci.insight.91353
38. MacFarlane EG, Parker SJ, Shin JY, Kang BE, Ziegler SG, Creamer TJ, Bagirzadeh R, Bedja D, Chen Y, Calderon JF, et al. Lineage-specific events underlie aortic root aneurysm pathogenesis in Loeys-Dietz syndrome. *J Clin Invest.* 2019;129:659–675. doi: 10.1172/JCI123547
39. Topouzis S, Majesky MW. Smooth muscle lineage diversity in the chick embryo. Two types of aortic smooth muscle cell differ in growth and receptor-mediated transcriptional responses to transforming growth factor-beta. *Dev Biol.* 1996;178:430–445. doi: 10.1006/dbio.1996.0229
40. Li DY, Brooke B, Davis EC, Mecham RP, Sorensen LK, Boak BB, Eichwald E, Keating MT. Elastin is an essential determinant of arterial morphogenesis. *Nature.* 1998;393:276–280. doi: 10.1038/30522
41. Curran ME, Atkinson DL, Ewart AK, Morris CA, Leppert MF, Keating MT. The elastin gene is disrupted by a translocation associated with supravalvular aortic stenosis. *Cell.* 1993;73:159–168. doi: 10.1016/0092-8674(93)90168-p
42. Shen YH, LeMaire SA. Molecular pathogenesis of genetic and sporadic aortic aneurysms and dissections. *Curr Probl Surg.* 2017;54:95–155. doi: 10.1067/j.cpsurg.2017.01.001
43. Lin CJ, Staiculescu MC, Hawes JZ, Cocciolone AJ, Hunkins BM, Roth RA, Lin CY, Mecham RP, Wagenseil JE. Heterogeneous cellular contributions to elastic laminae formation in arterial wall development. *Circ Res.* 2019;125:1006–1018. doi: 10.1161/CIRCRESAHA.119.315348
44. Verrecchia F, Mauviel A. Transforming growth factor-beta signaling through the Smad pathway: role in extracellular matrix gene expression and regulation. *J Invest Dermatol.* 2002;118:211–215. doi: 10.1046/j.1523-1747.2002.01641.x
45. Kimura N, Futamura K, Arakawa M, Okada N, Emrich F, Okamura H, Sato T, Shudo Y, Koyano TK, Yamaguchi A, et al. Gene expression profiling of acute type A aortic dissection combined with in vitro assessment. *Eur J Cardiothorac Surg.* 2017;52:810–817. doi: 10.1093/ejcts/ezx095
46. Pedroza AJ, Tashima Y, Shad R, Cheng P, Wirka R, Churovich S, Nakamura K, Yokoyama N, Cui JZ, Iosef C, et al. Single-cell transcriptomic profiling of vascular smooth muscle cell phenotype modulation in Marfan syndrome aortic aneurysm. *Arterioscler Thromb Vasc Biol.* 2020;40:2195–2211. doi: 10.1161/ATVBAHA.120.314670
47. Allaire E, Hasenstab D, Kenagy RD, Starcher B, Clowes MM, Clowes AW. Prevention of aneurysm development and rupture by local overexpression of plasminogen activator inhibitor-1. *Circulation.* 1998;98:249–255. doi: 10.1161/01.cir.98.3.249
48. Qian HS, Gu JM, Liu P, Kauser K, Halks-Miller M, Vergona R, Sullivan ME, Dole WP, Deng GG. Overexpression of PAI-1 prevents the development of abdominal aortic aneurysm in mice. *Gene Ther.* 2008;15:224–232. doi: 10.1038/sj.gt.3303069
49. DiMusto PD, Lu G, Ghosh A, Roelofs KJ, Su G, Zhao Y, Lau CL, Sadiq O, McEvoy B, Laser A, et al. Increased PAI-1 in females compared with males is protective for abdominal aortic aneurysm formation in a rodent model. *Am J Physiol Heart Circ Physiol.* 2012;302:H1378–H1386. doi: 10.1152/ajpheart.00620.2011
50. Otsuka G, Agah R, Frutkin AD, Wight TN, Dichek DA. Transforming growth factor beta 1 induces neointima formation through plasminogen activator inhibitor-1-dependent pathways. *Arterioscler Thromb Vasc Biol.* 2006;26:737–743. doi: 10.1161/01.ATV.0000201087.23877.e1
51. Samarakoon R, Higgins SP, Higgins CE, Higgins PJ. TGF-beta1-induced plasminogen activator inhibitor-1 expression in vascular smooth muscle cells requires pp60(c-src)/EGFR(Y845) and Rho/ROCK signaling. *J Mol Cell Cardiol.* 2008;44:527–538. doi: 10.1016/j.yjmcc.2007.12.006
52. Vaughan DE. PAI-1 and TGF-beta: unmasking the real driver of TGF-beta-induced vascular pathology. *Arterioscler Thromb Vasc Biol.* 2006;26:679–680. doi: 10.1161/01.ATV.0000209949.86606.c2
53. Edmondson DG, Lyons GE, Martin JF, Olson EN. Mef2 gene expression marks the cardiac and skeletal muscle lineages during mouse embryogenesis. *Development.* 1994;120:1251–1263.
54. Ito Y, Yeo JY, Chytil A, Han J, Bringas P Jr, Nakajima A, Shuler CF, Moses HL, Chai Y. Conditional inactivation of Tgfbr2 in cranial neural crest causes cleft palate and calvaria defects. *Development.* 2003;130:5269–5280. doi: 10.1242/dev.00708
55. Choudhary B, Ito Y, Makita T, Sasaki T, Chai Y, Sucov HM. Cardiovascular malformations with normal smooth muscle differentiation in neural crest-specific type II TGFbeta receptor (Tgfbr2) mutant mice. *Dev Biol.* 2006;289:420–429. doi: 10.1016/j.ydbio.2005.11.008
56. Zhou D, Feng H, Yang Y, Huang T, Qiu P, Zhang C, Olsen TR, Zhang J, Chen YE, Mizrak D, et al. hiPSC modeling of lineage-specific smooth muscle cell defects caused by TGFBR1A230T variant, and its therapeutic implications for Loeys-Dietz syndrome. *Circulation.* 2021;144:1145–1159. doi: 10.1161/CIRCULATIONAHA.121.054744
57. Cook JR, Clayton NP, Carta L, Galatioto J, Chiu E, Smaldone S, Nelson CA, Cheng SH, Wentworth BM, Ramirez F. Dimorphic effects of transforming growth factor-β signaling during aortic aneurysm progression in mice suggest a combinatorial therapy for Marfan syndrome. *Arterioscler Thromb Vasc Biol.* 2015;35:911–917. doi: 10.1161/ATVBAHA.114.305150
58. Rateri DL, Davis FM, Balakrishnan A, Howatt DA, Moorleghen JJ, O'Connor WN, Charnigo R, Cassis LA, Daugherty A. Angiotensin II induces region-specific medial disruption during evolution of ascending aortic aneurysms. *Am J Pathol.* 2014;184:2586–2595. doi: 10.1016/j.ajpath.2014.05.014
59. Sawada H, Chen JZ, Wright BC, Moorleghen JJ, Lu HS, Daugherty A. Ultrasound imaging of the thoracic and abdominal aorta in mice to determine aneurysm dimensions. *J Vis Exp.* 2019;145. doi: 10.3791/59013
60. Chen JZ, Sawada H, Moorleghen JJ, Weiland M, Daugherty A, Sheppard MB. Aortic strain correlates with elastin fragmentation in fibrillin-1 hypomorphic mice. *Circ Rep.* 2019;1:199–205. doi: 10.1253/circrep.CR-18-0012
61. Daugherty A, Rateri D, Hong L, Balakrishnan A. Measuring blood pressure in mice using volume pressure recording, a tail-cuff method. *J Vis Exp.* 2009;27:1291. doi: 10.3791/1291